Novel relations in massive gravity at Hawking-Page transition

Pavan Kumar Yerra[*] and Chandrasekhar Bhamidipati[†]
School of Basic Sciences, Indian Institute of Technology Bhubaneswar, Bhubaneswar, Odisha 752050, India

(Received 19 July 2021; accepted 22 October 2021; published 24 November 2021)

Sign and magnitude of Ruppeiner's curvature R_N is an empirical indicator of the respective nature and strength of microstructures of a thermodynamic system. We investigate the properties of R_N for black holes in massive gravity and show that the behavior of microstructures at the HP transition point is significantly altered by the graviton mass and horizon topology. In general, depending on the massive gravity parameters, R_N at HP transition point can be positive (negative) or even zero indicating respectively the dominance of repulsive (attractive) or non-interacting behaviors. In particular, presence of a weak repulsive type interaction is inferred in the large black hole branch at small pressures, which is new and in contrast to the known behavior of only attractive interactions for this branch in massless gravity. Further, when the graviton mass takes a critical value, the HP transition happens at zero temperature, where R_N turns out to be a universal constant, taking exactly the same value known for Schwarzchild black hole in AdS. Analysis of the geometry of general black holes in AdS close to the HP transition point via novel near horizon scaling limits, reveals the presence of fully decoupled Rindler spacetimes.

DOI: 10.1103/PhysRevD.104.104049

I. INTRODUCTION

Investigation of phase transitions in black holes has been a rich arena to explore as it has contributed immensely to our understanding of its microscopic and macroscopic properties. One of the celebrated transitions is of course the one proposed by Hawking and Page, which happens between a hot thermal gas and a stable large black hole in a Schwarzschild black hole in anti–de Sitter (AdS) spacetime [1]. The Hawking-Page (HP) phase transition has another interpretation due to AdS/CFT duality as a confinement/deconfinement transition in the boundary conformal field theory (CFT). In the black hole chemistry program [2–5], where the cosmological constant Λ is considered to be dynamical giving a pressure $P = -\Lambda/8\pi$, this can also be understood as a solid-liquid phase transition. For charged AdS black holes, there is also a critical region, where this first order phase transition ends in a second order one [6–8]. Both these phase transition points are meaningful and their investigation from a microsctopic as well as macroscopic point of view is still ongoing. Close to this critical region, the thermodynamic quantities of charged AdS black holes show special scaling behavior in terms of charge q, here Entropy $S \sim q^2$, Pressure $p \sim q^{-2}$, and Temperature $T \sim q^{-1}$ [8]. In a double scaling limit, where one approaches the near horizon region together with the large charge limit, the geometry turns out to be a fully decoupled d-dimensional Rindler space-time [9]. The emergence of decoupled space-times in the near horizon limit has given enormous insights in to the physics of branes and extremal black holes in general, through AdS/CFT dualities and might teach us novel issues from the CFT point of view.

There is also an alternative approach to study phase transitions, namely using Ruppeiner's thermodynamic geometry [10], which is a powerful diagnostic tool to know and classify the nature of competing microstructure interactions. The key quantity in this approach is the thermodynamic curvature, whose divergences typically reveal the points where the specific heat diverges, signally the presence of a critical point or phase transition. This method has been highly successful in understanding physics around critical points [11–17], especially in the context of extended thermodynamics. The analysis of thermodynamic curvature denoted as R_N, has revealed interesting phase structure of charged black holes in AdS, where some features of microstructures were expected to be similar to the van der Waals system, but do not hold [18–24]. For instance, analysis of R_N shows that, while an attractive microstructure interaction is dominant for most of the parameter regime, like the van der Waals system, there is also a contrasting feature, namely, the presence of a weak repulsive interaction for small black holes at high temperature [25]. There is a feature of thermodynamic curvature that has not been studied enough, that is its behavior close to a first order phase transition point as a naive application of the method does not show any divergence [26]. However, in the case

[*]pk11@iitbbs.ac.in
[†]chandrasekhar@iitbbs.ac.in

of a d-dimensional Schwarzschild black hole in AdS, it has recently been pointed out that R_N at the Hawking-Page transition point turns out to be a universal constant, depending only on the dimension of spacetime [27]. The universal constant thus defines a threshold, beyond which the repulsive interactions of radiation become attractive in nature aiding the formation of black holes[27]. An analogous calculation for the black holes in AdS with hyperbolic topology shows that R_N calculated for special zero mass solutions [28–30] turns out to be a universal constant along a renormalization group flow in dual conformal field theories [31].

The aforementioned developments motivate us to give a closer look at the HP transition point, in both d-dimensional Schwarzschild as well as corresponding black holes in general theories of gravity. The HP transition though is known to occur only when the horizon is spherical and thermodynamic geometry was reported in [27], limited to this case. In looking for existence of HP transition for arbitrary horizon topologies, an important class of examples is black holes in massive gravity theories. These theories have a remarkable feature which does not have a counterpart in even general Lovelock theories, i.e., the existence of HP transition as well as critical points in black hole solutions with Ricci flat or hyperbolic horizons, apart from the spherical horizon. Such black holes in AdS with nontrivial topology are called topological black holes. Though, thermodynamic geometry has been applied to this system before to study criticality [15,22,32], physics close to the HP transition point has not been explored yet. Brief motivations and developments in massive gravity theories are presented below, followed by a summary of our results and organization of the paper.

Einstein's general theory of relativity has been highly successful with experimental confirmation of several predictions, in particular, the recent observational evidence of LIGO collaboration [33,34] on gravitational waves. On the other hand, there are also important phenomena, for instance, accelerated expansion of the universe and the longstanding cosmological constant problem, among others, which suggest extensions to go beyond Einstein's theory. In this regard, an appealing extension involves massive graviton theories, motivated by hierarchy problems and their usefulness in quantum theory of gravity [35,36], which also seems to gel well with recent observations [37], putting novel lower limits on the graviton mass. Massive gravity theories have been historically important, which were explored starting from the early models proposed by Fierz and Paullo in 1939 [38], which went through various modifications with the advent of new ideas, such as, New massive gravites [39–42]. These theories have been actively studied in current literature [43–49]. Novel Black hole solutions, together with study of their thermodynamical properties [50–53] and applications to cosmology/astrophysics situations are also being explored with interest, to identify possible deviations from Einstein's theory [54–60]. An important class of massive gravity theories was proposed in [61], keeping holographic applications in mind and pointing out in particular that massive gravity may be stable and also free of ghosts [62], apart from the existence of black hole solutions [63–67]. There are other advantages. For instance, massive gravity theories hold promise in efforts to solve some of the mentioned problems in Einstein's theory as noted from [68–80]: such as, the possibility to explain the current observations coming from dark matter [81] and also relating to the accelerating expansion of universe without the requirement of any dark energy component [82,83]. It should be mentioned that attempts to embed massive gravities in string theory have been explored as well [84]. More importantly, it has been shown that van der Waals type liquid gas phase transitions and HP transition exist in the extended phase space approach as studied in a number of works in massive black hole chemistry [66,67,85–92]. Further, extension to the case of black hole solutions and the study of their microstructures in the case of bimetric gravity is expected to be interesting with novel observational constraints [93,94] and should be explored in the future.

We should also mention that the metric found in [61] is quite non-trivial and is in particular singular. The later feature is useful, as in this context the mass of the graviton can play a role identical to the one played by lattice in the holographic models of conductor: the conductivity in general consists of a Drude peak which in the massless gravity limit approaches a delta function. More clearly, nonlinear massive gravity theories need an auxiliary reference metric (which gives mass to gravitons) to get a Boulware-Deser ghost-free theory [34,49,95]. In principle, one can construct a special theory of massive gravity for each choice of reference metric, which can be nondegenerate [49]. On the other hand, in the context of gauge/gravity duality, massive gravity theories in AdS space with a singular (degenerate) reference metric (see equation-(2.4) are proposed to model a class of strongly interacting field theories with broken translational symmetry (i.e., momentum dissipation). For example, one can build a holographic model for normal conductors (having momentum dissipation) with finite **DC** conductivity [61,96], in contrast to massless gravity theories such as Einstein and Gauss-Bonnet ones with infinite **DC** conductivity [97–100]. Moreover, massive gravity theories with singular reference metric can effectively describe different phases of condensed matter systems with broken translational symmetry such as solids, liquids, (perfect) fluids [101–103], including applications to cosmological situations [104].

Summary and organization of the rest of the paper is as follows. The aim of this work is two fold. First is to investigate the behavior of thermodynamic curvature R_N at

the HP transition point and bring out the effect of graviton mass on nature of microstructures, in comparison to the massless case [27]. Second, is to report that a fully decoupled Rindler space time found earlier at the critical point in charged black holes [9], is remarkably present at the HP transition point too, in Schwarzschild as well corresponding neutral black holes in AdS in massive gravity. In this regard, in Sec. II, we start by writing down important thermodynamic relations for black holes in AdS in massive gravity theories, which is followed by the discussion of their phase structure, including the HP transition for various topologies in Sec. II A. Here, we point out an interesting feature for black holes with hyperbolic topology, which was noted earlier in the spherical topology case [105], namely the presence of a critical value of graviton mass $\hat{m}$, where the HP transition happens at zero temperature. In Sec. III, we start by obtaining a general line element on thermodynamic phase space with temperature and volume as fluctuating coordinates and use this to obtain an analytic expression for the associated thermodynamic curvature R_N. Analysis of thermodynamic curvature at the HP transition point, i.e., $R_N|_{HP}$, reveals novel features, which have no counter part in the massless limit of Einstein gravity. A contrasting feature is that the universal constancy of $R_N|_{HP}$ noted in [27], is explicitly broken in massive gravity. This is because in the current example, the nature as well as the strength of interaction, depends on horizon topology as well as varies drastically with massive gravity parameters at HP transition. In particular, there is a critical pressure (or cosmological constant value) depending on massive gravity parameters, which governs whether the microstructure interactions are effectively attractive, repulsive or in balance (a point where $R_N|_{HP}$ vanishes). Curiously, when the graviton mass reaches a critical value $\hat{m}$, the behavior of microstructures is found to be universal and identical to Schwarzschild black holes in AdS in massless gravity, as curvature $R_N|_{HP}$ becomes a universal constant independent of all parameters of the theory. Section IV, is devoted to exploring novel near horizon limits at the HP transition point of Schwarzschild black holes in AdS as well as their neutral counterparts with nontrivial topology in massive gravity theory, to show the existence of the decoupled Rindler geometry found earlier for charged systems in [9]. We end with a discussion of our findings in Sec. V.

II. ADS BLACK HOLES IN MASSIVE GRAVITY

Let us start with the action for a four dimensional theory of gravity with a negative cosmological constant Λ, together with mass term m for the graviton [66,85,106]:

$$I=-\frac{1}{16\pi}\int d^4x\sqrt{-g}\left(\mathcal{R}-2\Lambda+m^2\sum_i^4 c_i\mathcal{U}_i(g,f)\right). \quad (2.1)$$

Here, $\mathcal{R}$ is the Ricci scalar and c_i's are constants and f is a reference metric. The quantities $\mathcal{U}_i$'s are formed as symmetric polynomials of the eigenvalues of a 4×4 matrix $\mathcal{K}^\mu_\nu=\sqrt{g^{\mu\alpha}f_{\alpha\nu}}$, which are in turn given as:

$$\begin{aligned}\mathcal{U}_1&=[\mathcal{K}],\\ \mathcal{U}_2&=[\mathcal{K}]^2-[\mathcal{K}^2],\\ \mathcal{U}_3&=[\mathcal{K}]^3-3[\mathcal{K}][\mathcal{K}^2]+2[\mathcal{K}^3],\\ \mathcal{U}_4&=[\mathcal{K}]^4-6[\mathcal{K}^2][\mathcal{K}]^2+8[\mathcal{K}^3][\mathcal{K}]+3[\mathcal{K}^2]^2-6[\mathcal{K}^4]. \end{aligned} \quad (2.2)$$

It is well known that the above system admits static topological black hole solution, whose metric is given as [66,85,106]:

$$ds^2=-Y(r)dt^2+\frac{dr^2}{Y(r)}+r^2h_{ij}dx_idx_j, \quad (2.3)$$

where $f_{\mu\nu}$ appearing above stands for the reference metric:

$$f_{\mu\nu}=\mathrm{diag}(0,0,c_0^2h_{ij}). \quad (2.4)$$

Here, c_0 is a positive constant and $h_{ij}dx_idx_j$ is a spatial metric with constant curvature $2k$ and volume 4π, where i, $j=1,2$. The constant k can take different values, such as, $+1$, 0, or -1, in which cases, we obtain respectively black holes with horizons of topology, spherical, Ricci flat, or hyperbolic. As mentioned earlier, the reference metric in Eq. (2.4) breaks the diffeomorphism invariance of the theory in spatial directions (corresponds to momentum dissipation in dual field theory), but not along the radial and temporal directions (corresponds to conserved energy in dual field theory) [61]. Though the reference metric in Eq. (2.4) is singular, the theory is stable and ghost-free as it preserves the Hamiltonian constraint [48,49,107]. Thus, considering a particular form of reference metric $f_{\mu\nu}$ prescribed in [66,85], the $\mathcal{U}_i$'s are simplified to:

$$\mathcal{U}_1=\frac{2c_0}{r},\quad \mathcal{U}_2=\frac{2c_0^2}{r^2},\quad \mathcal{U}_3=0,\quad \mathcal{U}_4=0, \quad (2.5)$$

where now one can set $c_3=c_4=0$, as $\mathcal{U}_3=\mathcal{U}_4=0$. The lapse function $Y(r)$ is [66,85,106]:

$$Y(r)=k-\frac{m_0}{r}-\frac{\Lambda r^2}{3}+m^2\left(\frac{c_0c_1}{2}r+c_0^2c_2\right), \quad (2.6)$$

with the integration constant m_0 corresponding to the mass M of the black hole. The solution in Eq. (2.6), is asymptotically AdS and if the graviton mass term is dropped by setting $(m=0)$, it reduces to the Schwarzschild-AdS black hole for $k=+1$ [66,85]. We also note that the choice of the reference metric with graviton mass terms leave the solution with a Lorentz-breaking property [61]. It should also be mentioned that

the vacuum solution (obtained by setting $m_0 = 0$ in (2.6)] is not an AdS space unless graviton mass is zero, i.e., $m = 0$.

The thermodynamic quantities are given in terms of the horizon radius r_+, which is the largest positive root of $Y(r_+) = 0$. Especially, the temperature T, mass M and entropy S of the black hole are given as [66,85]:

$$T = \frac{Y'(r_+)}{4\pi} = \frac{k}{4\pi r_+} - \frac{r_+\Lambda}{4\pi} + \frac{m^2}{4\pi r_+}(c_0 c_1 r_+ + c_2 c_0^2), \tag{2.7}$$

$$M = \frac{m_0}{2} = \frac{r_+}{2}\left(k - \frac{\Lambda}{3}r_+^2 + m^2\left(\frac{c_0 c_1}{2}r_+ + c_0^2 c_2\right)\right), \tag{2.8}$$

$$S = \pi r_+^2. \tag{2.9}$$

In the extended thermodynamics approach, the pressure is provided by a dynamical cosmological constant,[1] as $p = -\frac{\Lambda}{8\pi} = \frac{3}{8\pi l^2}$ in four dimensions, with l being the AdS radius. The thermodynamic conjugate of p is the thermodynamic volume V. In this set up one identifies the mass M of the black hole with the enthalpy H [2], leading to the first law of black hole thermodynamics given as [66,85]:

$$dM = TdS + Vdp + \mathcal{C}_1 dc_1, \tag{2.10}$$

where

$$V = \left(\frac{\partial M}{\partial p}\right)_{S,c_1} = \frac{4\pi}{3}r_+^3, \tag{2.11}$$

$$\mathcal{C}_1 = \left(\frac{\partial M}{\partial c_1}\right)_{S,p} = \frac{c_0 m^2 r_+^2}{4}. \tag{2.12}$$

The specific heat at constant volume C_V, and at constant pressure C_p are found to be [106]:

$$C_V = T\left(\frac{\partial S}{\partial T}\right)_V = 0;$$
$$C_p = T\left(\frac{\partial S}{\partial T}\right)_p = 2S\left(\frac{8pS^2 + S(k + m^2 c_0^2 c_2) + \frac{m^2 c_0 c_1 S^{3/2}}{\sqrt{\pi}}}{8pS^2 - S(k + m^2 c_0^2 c_2)}\right). \tag{2.13}$$

[1]A scenario where cosmological constant is varying can occur in a gravity theory under various circumstances. For instance, in a situation where the theory is embedded in a larger set up consisting of other matter sectors, with possible origins in string theory. A dynamical cosmological constant can arise as a vev of a scalar field in a high energy theory under dimensional reduction, where there are several dynamical scalar fields with their respective potentials [108]. We do not pursue these aspects here.

A. Phase structure

From the expression of Hawking temperature (2.7), when

$$\epsilon \equiv (k + m^2 c_2 c_0^2), \tag{2.14}$$

is greater than zero, one can see that there exists a minimum temperature T_0 of the black hole, given by [85]

$$T_{\min} = T_0 = \sqrt{\frac{2\epsilon p}{\pi}} + \frac{m^2 c_0 c_1}{4\pi}, \tag{2.15}$$

with horizon radius $r_0 = \sqrt{\frac{\epsilon}{8\pi p}}$. For $T > T_0$, there exist a pair of black holes, small ($r_+ < r_0$) and large ($r_+ > r_0$), as shown in Fig. 1(a). The small black holes are thermodynamically unstable due to negative specific heat C_p, whereas the large black holes are stable with positive C_p, while C_p diverges for the black hole with horizon radius r_0 [See Fig. 1(b)].

As shown in Fig. 2(a), for $T < T_0$, no black holes can exist, except the vacuum phase characterized by vanishing free energy F. The large black holes are metastable having positive free energy when $T_0 < T < T_{HP}$, while at $T = T_{HP}$, the free energy of the large black hole equals to the vacuum free energy, where the Hawking-Page (HP) transition happens between the vacuum phase and large black hole phase. For $T > T_{HP}$, the large black hole phase having negative free energy is globally stable than vacuum phase [85].

The expressions for the free energy F and the Hawking-Page phase transition temperature T_{HP} are given by [85];

$$F = M - TS = \frac{r_+}{4}\left(\epsilon - \frac{8\pi p}{3}r_+^2\right), \tag{2.16}$$

$$T_{HP} = \sqrt{\frac{8\epsilon p}{3\pi}} + \frac{m^2 c_0 c_1}{4\pi}. \tag{2.17}$$

The Hawking-Page phase transition happens at the horizon radius $r_{HP} = \sqrt{\frac{3\epsilon}{8\pi p}}$. The phase structure, as shown in Fig. 2(b), is identical to that of the Schwarzschild-AdS black holes with spherical topology ($k = +1$) of massless graviton case [27,109]. Thus, provided $\epsilon > 0$, the presence of massive graviton admits the Hawking-Page transition for the black holes with topology flat ($k = 0$) and hyperbolic ($k = -1$) as well, unlike the case of massless graviton, where only the black holes with spherical topology ($k = +1$) can under go Hawking-Page transition [85,110].

From Eq. (2.17), one notes the possibility of having the HP transition at zero temperature for specific choice of parameters. Such a phenomenon in case of black holes with spherical topology, where the dual field theory also

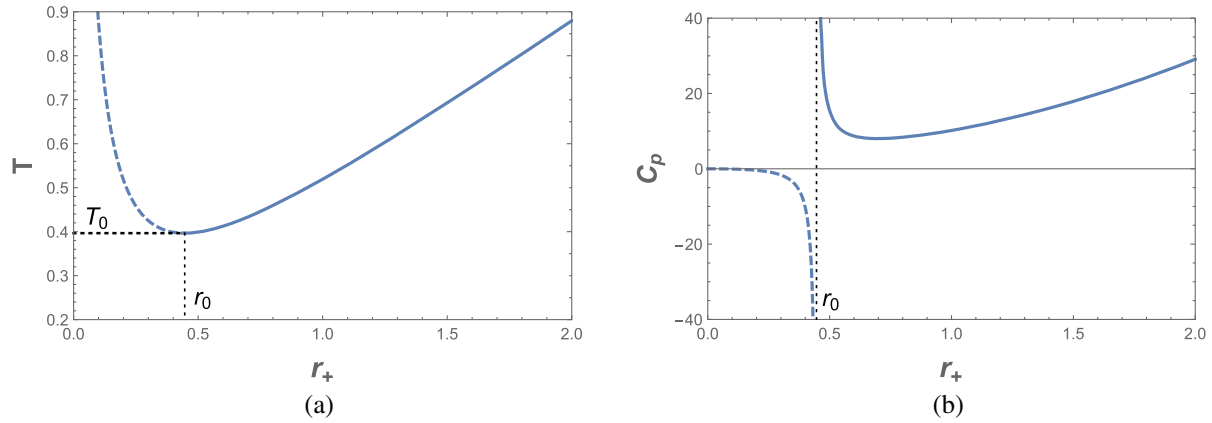

FIG. 1. For the topological AdS black holes in massive gravity (a) Temperature T versus horizon radius r_+ plot, indicating the existence of minimum temperature T_0 at r_0, when $\epsilon \equiv (k + m^2 c_2 c_0^2) > 0$. For $T < T_0$, no black holes can exist, except the vacuum phase. For $T > T_0$, there exist small (shown with dashed blue curve) and large (shown with solid blue curve) black holes. (b) Specific heat C_p versus r_+ plot, indicating the negative C_p for small black holes (dashed blue curve), positive C_p for large black holes (solid blue curve), and C_p diverges for the black hole with horizon radius r_0. (Here, the parameters $k = -1$, $m = c_0 = 1$, $c_1 = 0.5$, $c_2 = 2$, $p = 0.2$, are used. Similar behavior is observed for other topologies.).

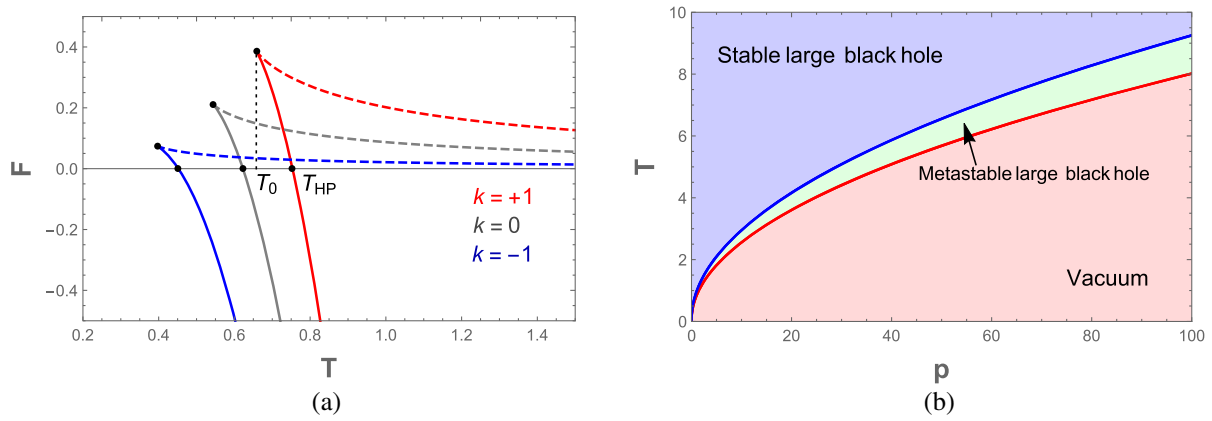

FIG. 2. For the topological AdS black holes in massive gravity (a) Free energy F versus Temperature T plot at various horizon topologies k for a fixed pressure $p = 0.2$. Dashed curve indicates the small black hole branch, solid curve indicates the large black hole branch, T_0 is the minimum temperature and T_{HP} is the Hawking-Page phase transition temperature. (b) Phase structure in T–p plane for horizon topology $k = -1$ (Similar phase structure is observed for other topologies). The red and blue curves respectively correspond to the black hole minimum temperature T_0 and the HP phase transition temperature T_{HP}. (Here, the parameters $m = c_0 = 1$, $c_1 = 0.5$, $c_2 = 2$, are used.).

undergoes deconfinement transition at zero temperature was already noted earlier in a specific holographic massive gravity model [105]. This is plotted in Fig. 3(a) and corresponds to the case with $c_1 = 0$. The presence of graviton mass in the bulk breaks the translational invariance and was argued to encode the rate of momentum dissipation in the dual field theory. There is a new length scale in the theory set by $l_m \approx 1/m$, which determines the distance which the particles travel before shedding momentum. At a critical value of graviton mass $\hat{m}^2$, the momentum dissipation effects are strong and the critical temperature for deconfinement is driven to zero. Here, one can also set the graviton mass to zero and recover the usual HP transition for Schwarzschild black holes in AdS. For generic horizon topology in the bulk, the point where the HP transition temperature goes to zero for different possible choices of parameters and graviton mass can be studied, but there are some differences. For instance, one can consider $c_1 < 0$ where naively the HP transition temperature does approach zero, but since the vacuum solution here contains horizons, this case is not suitable (arguments are similar to the ones given in [105]). The case with $c_1 = 0$ discussed above is more interesting as seen from Figs. 3(a) and 3(b) for black holes with spherical and hyperbolic topology respectively. The curves indicate the line of first order transition separating the vacuum and black hole phases, with HP

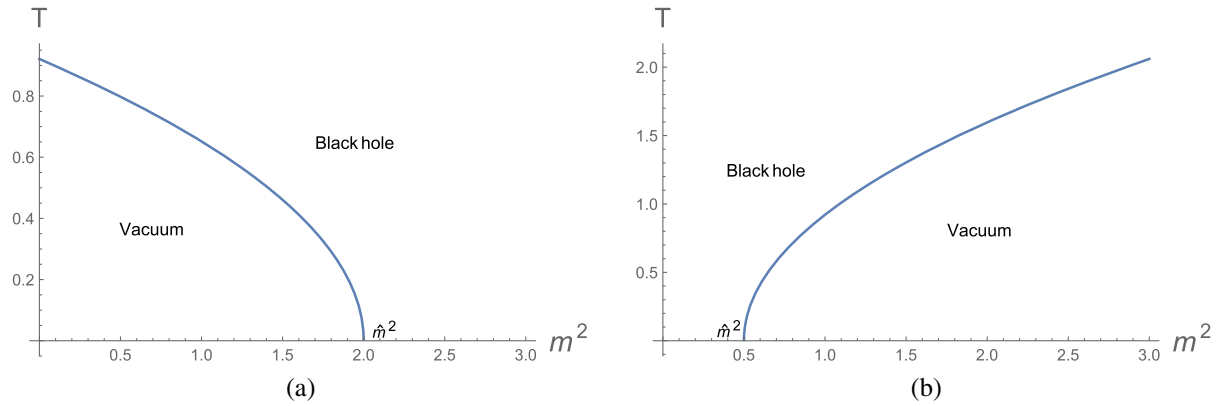

FIG. 3. The phase diagram in the case of massive coefficient $c_1 = 0$, showing that the Hawking-Page transition temperature $T_{HP}(m^2)$ vanishes at $m^2 = \hat{m}^2 = -k/(c_2 c_0^2)$ for the black holes with a) spherical horizon topology (Here, the parameters $p = c_0 = 1$, $c_2 = -1/2$, are used matching [105]), b) hyperbolic horizon topology (Here, the parameters $p = c_0 = 1$, $c_2 = 2$, are used). The first order phase transition line terminates in a second order transition point at zero temperature and $m^2 = \hat{m}^2$.

transition driven to zero temperature at a critical value of graviton mass, $\hat{m}^2 = -k/(c_2 c_0^2)$. Notice that in the hyperbolic topology case, there is no HP transition phenomena if the graviton mass is set to zero as the system is dominated by a black hole at all temperatures. With nonzero graviton mass, the HP transition happens and the dual field theory confines beyond the critical value $\hat{m}^2$, as seen in Fig. 3(b). This is opposite to the behavior in spherical horizon topology case. All these are interesting effects and it is important to understand the behavior of microstructures in some of these special limits. The plan of the next two sections is to gather empirical information from thermodynamic curvature, especially as m^2 approaches $\hat{m}^2$, as well as explore the geometry around the HP transition point in general, in novel near horizon limits.

III. THERMODYNAMIC CURVATURE AT THE HP TRANSITION POINT

Thermodynamic or Ruppeiner geometry can be thought of as a macroscopic approach to gain understanding about the microscopic aspects of a thermodynamic system, where a thermodynamic curvature scalar carries much information about the type of interactions. Thermodynamic geometry has its roots in fluctuation theory, which starts from studying the inverse of Boltzman entropy formula, namely:

$$\Omega = e^{\frac{S}{k_B}}, \tag{3.1}$$

where Ω stands for the number of microstates, S is the entropy and k_B is the Boltzmann constant. One starts by considering a large thermodynamic system I_0 in equilibrium, that consists in it a subsystem I, with the later having, say, two independent fluctuating coordinates, x^i where $i = 1, 2$. The probability $P(x^1, x^2)$ of having the state of the system between (x^1, x^2) and $(x^1 + dx^1, x^2 + dx^2)$ can straightforwardly be related to the number of microstates Ω from Eq. (3.1). In this situation, the second law of thermodynamics states that the pair (x^1, x^2) are frozen on the values which maximize the entropy $S = S_{\max}$. In other words, the pair (x^1, x^2) actually describes thermodynamic fluctuations around this maximum. One can now expand the entropy about this maximum up to second order, which shows that the probability is [10]:

$$P(x^1, x^2) \propto e^{-\frac{1}{2}\Delta l^2}. \tag{3.2}$$

Now,

$$\Delta l^2 = -\frac{1}{k_B}\frac{\partial^2 S}{\partial x^i \partial x^j}\Delta x^i \Delta x^j, \tag{3.3}$$

stands for the line element, which is a measure of the thermodynamic distance between two neighborhood fluctuating states. If the distance between these states is shorter, the more probable is the fluctuation between them. Based on various studies of the thermodynamic curvature R, following from the metric in Eq. (3.3) for various fluid/gas systems, such as ideal and van der Waals systems, Fermi/Bose systems including quantum gases, the empirical understanding gained can be summarized as follows: A negative (positive) sign of R indicates that attractive (repulsive) type interactions are dominant in the system. Furthermore, a larger negative (positive) value of curvature signifies that the system is less (more) stable, which further points toward the stability of Bose (Fermi) type systems [111–115]. The divergences of R indicate the presence of critical points and vanishing of curvature is suggestive of balance of repulsive and attractive interactions, namely, a noninteractive situation.

To obtain the thermodynamic curvature, the line element in Eq. (3.3) needs to be computed for a choice of fluctuation coordinates. In the current situation where entropy is clearly the key thermodynamic quantity, the line element

can be obtained by starting from the internal energy $U = U(S, V)$. We have the first law $dU = TdS - PdV$, which can be written as:

$$dS = \frac{1}{T}dU + \frac{P}{T}dV, \tag{3.4}$$

with V representing the thermodynamic volume, conjugate to pressure $P = -\Lambda/8\pi G$ [2,3,116]. We now take the fluctuating variables to be $(x^1 = T, x^2 = V)$, in which case the line element can be written explicitly as [18,25,117]:

$$dl_U^2 = \frac{1}{T}\left(\frac{\partial S}{\partial T}\right)\Big|_V dT^2 - \frac{1}{T}\left(\frac{\partial P}{\partial V}\right)\Big|_T dV^2, \tag{3.5}$$

which can be also be written in a useful form as:

$$dl^2 = \frac{C_V}{T^2}dT^2 - \frac{1}{T}\left(\frac{\partial p}{\partial V}\right)_T dV^2. \tag{3.6}$$

At this stage, the metric in Eq. (3.6) is quite general and any thermodynamic system (not necessarily a black hole) can be studied by computing the associated curvature from it. Microstructures of van der Waals liquid-gas system studied from the curvature coming from the line element in Eq. (3.6) reveal a completely coherent and clear picture of the nature of interactions [25]. For some specific case of static black holes in AdS [6,8], additional normalization of the thermodynamic curvature may be required to extract the nature of interactions of microstructures [18,25]. This can be seen from the fact $(\frac{\partial S}{\partial T})_V = C_V/T$ is zero from equation (2.13), translating to the metric being noninvertible. One can deal with this situation by momentarily assuming C_V to a small non zero quantity and as the $k_B \to 0^+$ limit [18,25]. The curvature R can now be computed and C_V comes to be a overall multiplicative constant in it. One can rescale to remove the dependence on C_V and define a new curvature as $R_N = RC_V$, which carries the same empirical information as R and gives consistent results for black holes [18,25,26].

To proceed further, we use $p = -\frac{\Lambda}{8\pi}$ to invert Eq. (2.7) and obtain the expression for equation of state $p(V, T)$ as:

$$p = \frac{1}{8\pi}\left\{\frac{(4\pi T - m^2 c_0 c_1)}{(\frac{3V}{4\pi})^{\frac{1}{3}}} - \frac{(k + m^2 c_2 c_0^2)}{(\frac{3V}{4\pi})^{\frac{2}{3}}}\right\}. \tag{3.7}$$

Using the above expression in Eq. (3.6) and with a suitable normalization taking C_V to be a constant as discussed above, on obtains:

$$R_N = \frac{(2\epsilon(36\pi)^{\frac{1}{3}} + 3c_0c_1m^2V^{\frac{1}{3}})(2\epsilon(36\pi)^{\frac{1}{3}} - 24\pi TV^{\frac{1}{3}} + 3c_0c_1m^2V^{\frac{1}{3}})}{2(2\epsilon(36\pi)^{\frac{1}{3}} - 12\pi TV^{\frac{1}{3}} + 3c_0c_1m^2V^{\frac{1}{3}})^2}. \tag{3.8}$$

Let us start by mentioning that in the limit where the graviton mass is set to zero, and for black holes with spherical topology $(k = +1)$, Eq. (3.8) reproduces the result for thermodynamic curvature in [27] and is also consistent with [22] in the appropriate limit. For the present case, R_N diverges for the black hole with minimum temperature and this is consistent with the picture that the specific heat at constant pressure in Eq. (2.13) also diverges at this point. Since the small black hole branch is unstable, we do not pursue this branch further. For the large black hole branch, R_N is finite and its sign depends on the sign of the massive gravity coefficient c_1. For $c_1 \geq 0$, as shown in Fig. 4, R_N is negative for the large black hole branch, indicating the dominance of attractive interactions for both metastable and stable large black holes, irrespective of horizon topology.

For $c_1 < 0$, R_N shows an interesting behavior, namely, it can be positive, negative and also vanish in the large black hole branch, i.e., there can respectively be repulsive, attractive and non-interacting situations, in both metastable and stable large black hole branches (See Fig. 5). If the metastable branch is ignored, then the divergent behavior of R_N can also be dropped and one can start discussing the physical behavior of microstructures beginning from the HP transition point. This can be done by plugging the corresponding temperature and thermodynamic volume in Eq. (3.8) obtaining a curious result,

$$R_N|_{HP} = -\left(\frac{3}{2} + \frac{c_0c_1m^2}{4}\sqrt{\frac{6}{\pi\epsilon p}} + \frac{1}{8}\left(\frac{c_0c_1m^2}{4}\sqrt{\frac{6}{\pi\epsilon p}}\right)^2\right). \tag{3.9}$$

Setting $m = 0$ in the above equation and taking $(k = +1)$ for spherical topology $R_N|_{HP}$ is a negative constant $(-3/2)$, matching the claim in [27] that for AdS Schwarzschild black holes thermodynamic curvature is a universal constant. For the AdS Schwarzschild case, R_N is positive for thermal AdS and negative for the black hole at the HP transition point, where the microstructure interactions show a crossover behavior from repulsive type to attractive type as the stable large black hole is formed. However, this process is expected to be more involved in the present case, as from Eq. (3.9) R_N is no longer a constant. There is explicit dependence on pressure p and other parameters of the system even at HP transition point, and hence the universal constancy nature of thermodynamic curvature is broken by the graviton mass terms. Further, in contrast to

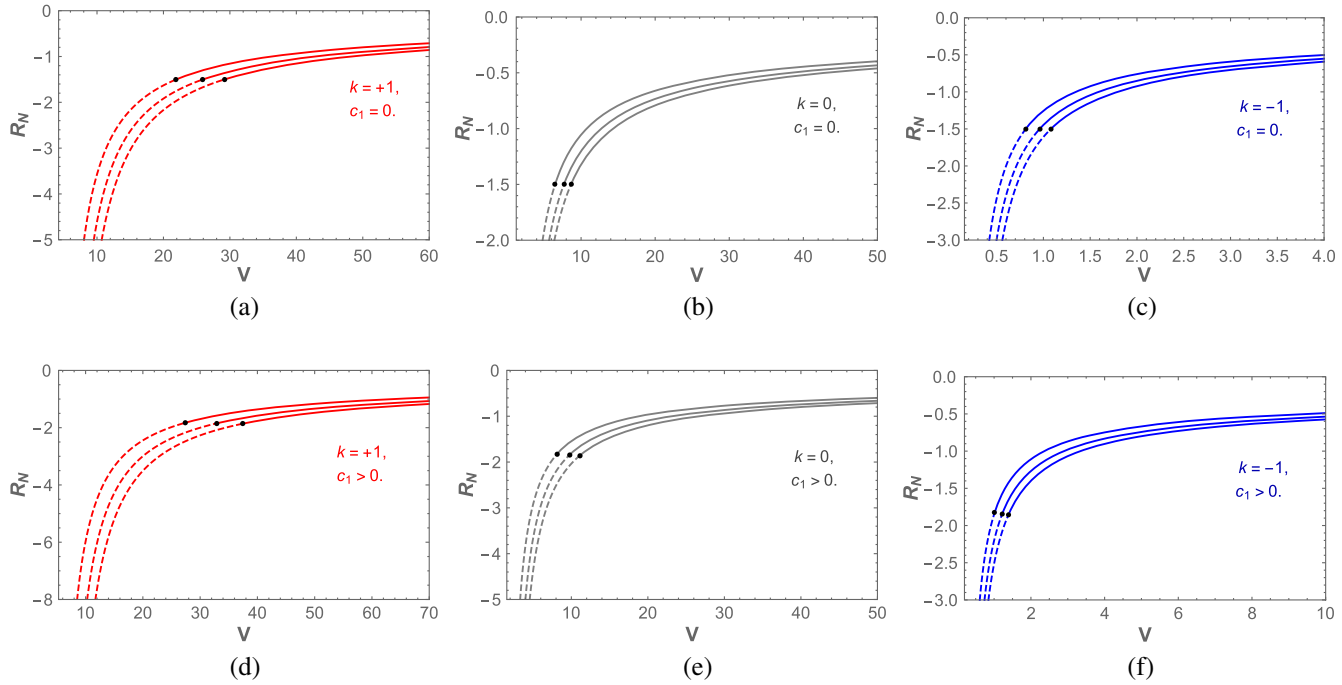

FIG. 4. In the case of massive coefficient $c_1 \geq 0$, the normalized scalar curvature R_N as a function of thermodynamic volume V for T = 0.5, 0.52, 0.55 from bottom to top, at various horizon topologies k. The dashed and solid curves are for the metastable and stable large black holes, respectively, while the black color dots represent HP transition points. (Here, the parameters $m = c_0 = 1$, $c_1 = 0.5$, $c_2 = 2$, are used.).

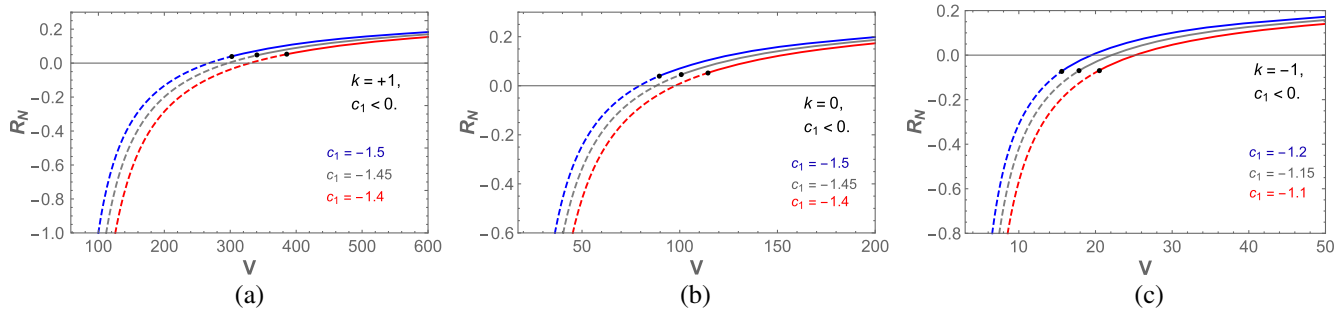

FIG. 5. In the case of massive coefficient $c_1 < 0$, the normalized scalar curvature R_N as a function of thermodynamic volume V for T = 0.1, 0.105, 0.11 from bottom to top, at various horizon topologies k. The dashed and solid curves are for the metastable and stable large black holes, respectively, while the black color dots represent HP transition points. (Here, the parameters $m = c_0 = 1$, $c_2 = 2$, are used.).

[27], where only the attractive type interactions are found at this point for spherical topology case, there are more general possibilities here. Although, the graviton mass significantly alters the behavior of microstructures, for $T = 0$ one still gets $R_N = \frac{1}{2}$, which signifies repulsive type interaction, irrespective of horizon topology and graviton mass (see also [31] for related discussion). From Eq. (3.9) for the case $c_1 \geq 0$, the nature of microstructures changes from repulsive to attractive type beyond HP transition point, as suggested by $R_N|_{HP}$, in accordance with the massless graviton case [27]. The novel result is in the case with $c_1 < 0$ (See Fig. 6) which surprisingly reveals that $R_N|_{HP}$ apart from being negative, can also be positive or even vanish at HP transition point. Since, HP transition is a threshold for formation of stable large black holes, microscopically, the corresponding process in massive gravity is expected to be quite nontrivial than the case of Schwarzschild black holes in Einstein gravity.

The point where the crossover happens is obtained from

$$R_N|_{HP} = 0 \Rightarrow p = \frac{3c_0^2 c_1^2 m^4}{32\pi\epsilon} \equiv p^*. \tag{3.10}$$

Thus, for $p > (<) p^*$, the effective interactions at the HP transition point are attractive (repulsive). Such crossover points are of profound significance as is evident from

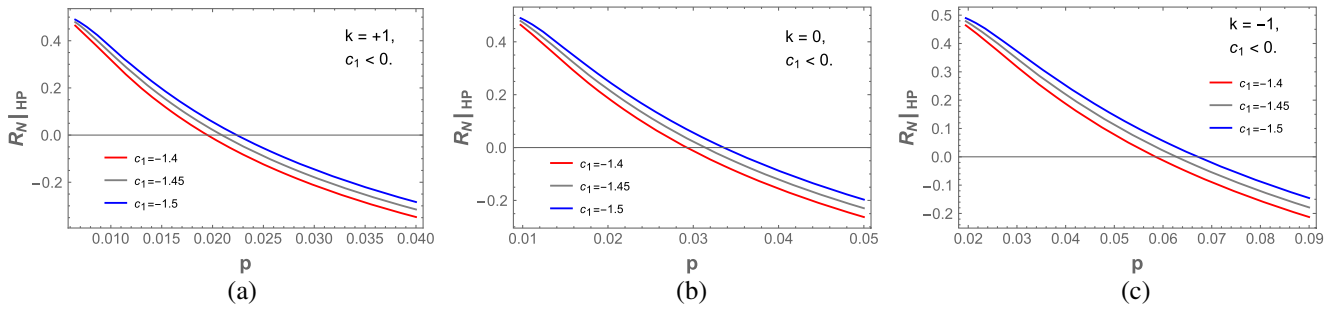

FIG. 6. In the case of massive coefficient $c_1 < 0$, for various horizon topologies k, the normalized scalar curvature at HP transition point (i.e., $R_N|_{HP}$) as a function of pressure p shows the sign changing behavior. (Here, the parameters $m = c_0 = 1$, $c_2 = 2$, are used.).

earlier of charged black holes in AdS, where they give the sign-changing curve at a temperature half of the spinodal temperature [25]. These zero crossings of R_N thus corresponding to shift in balance of interaction type and change in microstructure behavior of the black hole. We now consider one possible interpretation for the result in Eq. (3.10) in the present case. As seen from Fig. 6 the curves for $R_N|_{HP}$ start out as positive with value close to the $T = 0$ value, i.e., 0.5 and decrease further at higher pressures, eventually becoming negative after p^*. One thus infers that in the presence of massive graviton, there is a special situation for the black hole at HP transition point which has no counterpart in the massless gravity case. That is, $R_N|_{HP}$ is positive at small pressures where the microstructure interactions are effectively repulsive, which is a new feature for large black holes, although these interactions are weaker than the corresponding ones of the vacuum solution (as the absolute value of curvature is smaller).

Having learned about the nature of interactions at the HP transition point, one can also comment on their strength, which can be inferred from the magnitude $|R_N|_{HP}|$ for two different ranges of the parameter c_1. From Eq. (3.9), when the massive coefficient $c_1 > 0$, $|R_N|_{HP}|$ is highest for hyperbolic topology, followed by flat and spherical topology, i.e.,

$$|R_N|_{HP}|_{(k=-1)} > |R_N|_{HP}|_{(k=0)} > |R_N|_{HP}|_{(k=+1)}. \quad (3.11)$$

However, when the massive coefficient $c_1 < 0$ and for a certain range of parameters, the above order can be reversed, i.e., $|R_N|_{HP}|_{(k=-1)} < |R_N|_{HP}|_{(k=0)} < |R_N|_{HP}|_{(k=+1)}$. Some values of $c_1 < 0$ and possible range of pressures where this happens are shown in Fig. 7.

Towards the end of Sec. II A, possibility of HP transition at zero temperature was noted at a critical value of graviton mass $\hat{m}^2$. The Ruppeiner scalar for the black holes with spherical and hyperbolic horizons at this zero temperature HP transition turns out to be $R_N^{(T_{HP}=0)}|_{HP} = -3/2$ (from Eq. (3.9)), matching the value found in the massless graviton limit [27]. This is a universal constant independent of horizon topology, other parameters and also graviton mass. Thus, the d-dimensional value of $R_N^{(T_{HP}=0)}|_{HP}$ at $\hat{m}^2$ is also expected to be a universal negative constant (depending only on the space-time dimension), taking exactly the same value known for d-dimensional Schwarzschild black hole in AdS [27]. A possible explanation is that the nature of microstructure behavior at this special point even in the presence of massive graviton is expected to similar to Schwarzschild case, i.e., repulsive interactions becoming attractive beyond HP transition.

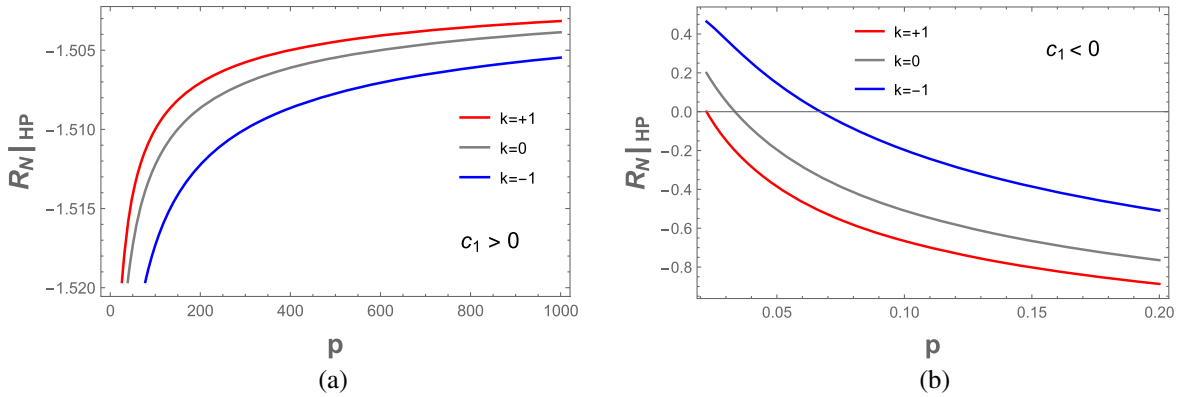

FIG. 7. The effect of horizon topology k on the strength of interactions at HP transition point (i.e., on $|R_N|_{HP}|$), (a) for the massive coefficient $c_1 > 0$, and (b) for the massive coefficient $c_1 < 0$. (Here, the parameters $m = c_0 = 1$, $c_1 = -1.5$, $c_2 = 2$, are used.).

IV. DECOUPLED GEOMETRY AT THE HP TRANSITION POINT

In this section, we take a closer look at the geometry near the HP transition point in Schwarzschild black holes in AdS and then generalize the results to corresponding solutions in massive gravity theory. Let us first compare the scaling of various quantities for charged and neutral black holes in AdS, at the second order critical point and HP transition point with respective parameters, as shown below.

Charged AdS black holes at critical point	Schwarzschild-AdS black holes at HP transition point
$r_{cr} \sim q^{1/(D-3)}$,	$r_{\rm HP} \sim l$,
$T_{cr} \sim q^{-1/(D-3)}$,	$T_{\rm HP} \sim l^{-1}$,
$p_{cr} \sim q^{-2/(D-3)}$.	$p_{\rm HP} \sim l^{-2}$.

Here D is the space-time dimension. Scaling of thermodynamic quantities at the HP transition point[2] with respect to AdS length l [109] is similar to the scaling with respect to the charge $q^{1/(D-3)}$ at the critical point [8,9]. For charged black holes in AdS, the proposal in [9] is that, as the critical point is approached in a large charge limit together with a near horizon limit, the black hole geometry decouples in to a d-dimensional Rindler space-time. Now, in the case of Schwarzschild black holes in AdS, an analogous double scaling limit at the HP transition point can now be thought of as the limit in which $l \to \infty$ taken together with the near horizon limit. To see this, consider the metric of the d-dimensional Schwarzschild-AdS black hole geometry [118]:

$$ds^2 = -Y(r)dt^2 + \frac{dr^2}{Y(r)} + r^2 d\Omega^2_{D-2}, \tag{4.1}$$

where the lapse function is

$$Y(r) = 1 - \frac{16\pi M}{(D-2)\omega_{D-2}}\frac{1}{r^{D-3}} + \frac{r^2}{l^2}, \tag{4.2}$$

and ω_{D-2} is the volume of the round S^{D-2} surface. Naively, taking the $l \to \infty$ on the above black hole solution in Eq. (4.2), will give us the corresponding solution in flat space-time, whose near horizon limit is the well known Rindler$_2 \times S^{D-2}$. Instead, by writing $r = r_+ + \eta\sigma$ and $t = \tau/\eta$ and for small η, the metric for the Schwarzschild-AdS black holes at the HP transition point becomes,

$$ds^2 = -\left(\frac{\sigma Y'(r_+)}{\eta}\right)d\tau^2 + \frac{1}{\left(\frac{\sigma Y'(r_+)}{\eta}\right)}d\sigma^2 + (r_+^2 + 2\eta\sigma r_+)d\Omega^2_{D-2}, \tag{4.3}$$

where, $Y(r = r_+) = 0$ and $Y' = \frac{dY(r)}{dr}|_{(\rm r=r+)} = 4\pi T$. Now, at the HP transition point, we have $T = T_{\rm HP} = \frac{(D-2)}{2\pi l}$ and $r_+ = r_{\rm HP} = l$ [109,118]. We can now take a new double scaling limit by approaching the horizon in the limit $\eta \to 0$, while at the same time taking the limit $l \to \infty$, by holding $l\eta = \tilde{l}$ fixed. Then the metric (4.3) becomes:

$$ds^2 = -(4\pi\tilde{T}_{\rm HP})\sigma d\tau^2 + \frac{1}{(4\pi\tilde{T}_{\rm HP})}\frac{d\sigma^2}{\sigma} + d\mathbb{R}^{D-2}, \tag{4.4}$$

where, $\tilde{T}_{\rm HP} = T_{\rm HP}/\eta$. Also, in the limit $l \to \infty$, the cosmological constant $\Lambda = 0$, and the metric on the round S^{D-2} becomes flat (as the radius $r_{\rm HP}$ of S^{D-2} diverges). Thus, the metric (4.4) represents the line element for fully decoupled (as the throat length diverges) D-dimensional Rindler space-time with zero cosmological constant, exactly analogous to the one uncovered for the charged AdS black holes at critical point in [9]. The Rindler space-time obtained here is also different from the standard Rindler$_2 \times S^{D-2}$ that one gets as the near horizon limit of general non-extremal black holes.

The extension of above results to the case of massive gravity in 4-dimensions [85,119] can be implemented in an analogous manner, as the similarity in the scaling of thermodynamic quantities at the critical point with respect to charge, and, with respect to AdS length at the HP transition point, continues to hold, as seen below:

Charged topological AdS black holes in massive gravity at critical point	Topological-AdS black holes in massive gravity at HP transition point
$r_{cr} = \sqrt{\frac{6}{\epsilon}}q$,	$r_{\rm HP} = l\sqrt{\epsilon}$,
$T_{cr} = \frac{\epsilon^{\frac{3}{2}}}{3\sqrt{6}\pi q} + \frac{m^2 c_0 c_1}{4\pi}$,	$T_{\rm HP} = \frac{\sqrt{\epsilon}}{\pi l} + \frac{m^2 c_0 c_1}{4\pi}$,
$p_{cr} = \frac{\epsilon^2}{96\pi q^2}$.	$p_{\rm HP} = \frac{3}{8\pi l^2}$.

Here, ϵ is defined in Eq. (2.14). To examine the near horizon geometry for topological AdS black hole in massive gravity at HP transition point, the metric in (2.3) with corresponding values inserted becomes:

$$ds^2 = -\left(\frac{4\pi\sigma T_{\rm HP}}{\eta}\right)d\tau^2 + \frac{1}{\left(\frac{4\pi\sigma T_{\rm HP}}{\eta}\right)}d\sigma^2 + (r_{\rm HP}^2 + 2\eta\sigma r_{\rm HP})h_{ij}dx_i dx_j. \tag{4.5}$$

One can take the near horizon limit $\eta \to 0$ while at the same time keeping l large, by holding $l\eta = \tilde{l}$ fixed. However, in addition to these limits, looking at the form of $T_{\rm HP}$ in equation (2.17) one also needs to take the limit $c_1 \to 0$ to get a consistent near horizon metric, for the case of arbitrary topology.[3] Thus, the metric in (4.5) then goes over to:

[2]Schwarzschild-AdS black holes at minimum temperature T_0 also show the same scaling behavior as present at HP transition point, which has in fact been used to propose a type of holographic duality in [27]

[3]If instead, one takes the $m \to 0$ or $c_0 \to 0$, then, due to the requirement of $\epsilon > 0$ in Eq. (2.17), HP transition point ceases to exist for arbitrary topology.

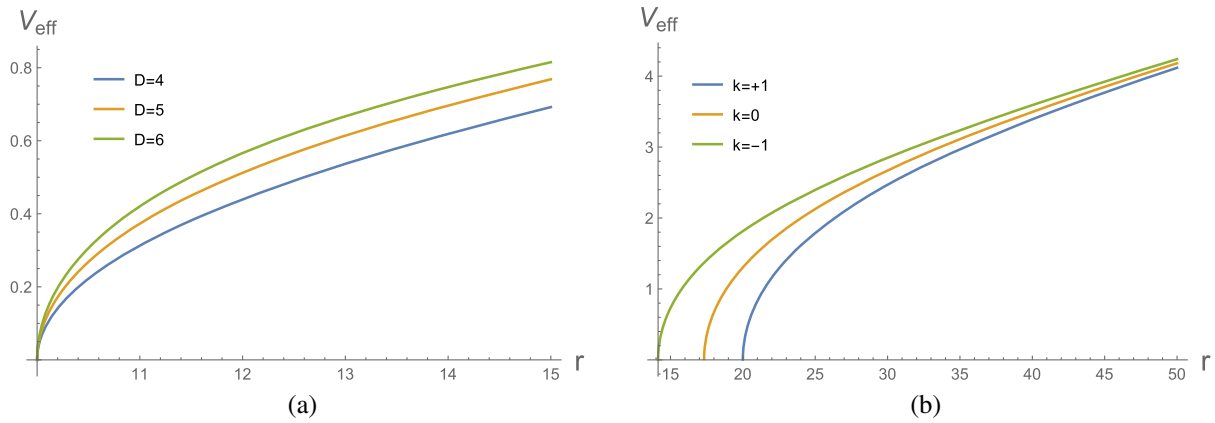

FIG. 8. The effective potential V_{eff} with $L = 0$, $l = 10$, and $\mu = 0.5$, showing the absence of local minimum (a) Schwarzschild-AdS black holes in various space-time dimensions D, (b) 4-dimensional topological AdS black holes in massive gravity at various topologies k (Here, the parameters $m = c_0 = 1$, $c_1 = 2$, $c_2 = 3$, are used.).

$$ds^2 = -(4\pi\tilde{T}_{\text{HP}})\sigma d\tau^2 + \frac{1}{(4\pi\tilde{T}_{\text{HP}})}\frac{d\sigma^2}{\sigma} + d\mathbb{R}^2, \tag{4.6}$$

where, $\tilde{T}_{\text{HP}} = T_{\text{HP}}/\eta$, and both $l\eta = \tilde{l}$ and $c_1/\eta = \tilde{c}_1$ are held fixed. This new triple scaling limit results in a completely decoupled Rindler space-time with zero cosmological constant, matching the one obtained for charged black hole at critical point in [120]. One also notes that a $l \to \infty$ limit cannot be taken in the case when the massive coefficient c_1 is negative, as the temperature in this limit takes the value $T_{\text{HP}} = \frac{c_0 c_1 m^2}{4\pi}$, which is unphysical [119]. Thus, when c_1 is negative, a non-trivial near horizon limit as discussed above, which gives a decoupled geometry as in [9], does not in general exist.

There is one other way to inspect the geometry of black holes at the HP transition point, by studying the behavior of probe particles in its background. For instance, for the case of charged AdS black hole at the critical point, such a study was performed in [9], which gives information about the stability of the system. Following the methods in [9,121,122], the effective potential for the motion of a point particle of mass μ moving in the background of the Schwarzschild-AdS black hole at the HP transition point is

$$V_{\text{eff}}(r) = \sqrt{Y_{\text{HP}}(r)}\sqrt{\mu^2 + \frac{L^2}{r^2}}, \tag{4.7}$$

where the lapse function is

$$Y_{\text{HP}}(r) = 1 - \frac{16\pi M_{\text{HP}}}{(D-2)\omega_{D-2}}\frac{1}{r^{D-3}} + \frac{r^2}{l^2}, \tag{4.8}$$

and

$$M_{\text{HP}} = \frac{(D-2)\omega_{D-2}}{8\pi} l^{D-3}, \tag{4.9}$$

with L denoting the angular momentum of the particle. The effective potential in equation (4.7), which may generally have a minimum at some value of r_{min} ($> r_{\text{HP}}$), depending on the values taken by μ and L. It was argued in [9], that the presence of such a local minimum for a test particle at rest would lead to a condensation and possibly an instability of the black hole. As can be seen from Fig. 8(a), there is no local minimum and the potential is purely attractive type binding all the subsystems that make up the black hole together. A similar analysis can be repeated for topological AdS black hole in massive gravity at the HP transition point, considering the effective potential (4.7) of the probe with (using equation (2.6),

$$Y_{\text{HP}}(r) = k - \frac{2M_{\text{HP}}}{r} + \frac{r^2}{l^2} + m^2\left(\frac{c_0 c_1}{2}r + c_0^2 c_2\right), \tag{4.10}$$

and

$$M_{\text{HP}} = l\epsilon\left(\sqrt{\epsilon} + \frac{m^2 c_0 c_1}{4} l\right). \tag{4.11}$$

Fig. 8(b) confirms that there is no instability.

V. CONCLUSIONS

In this paper, we considered the 4-dimensional topological AdS black holes in massive gravity, where the presence of massive graviton admits the Hawking-Page transition for the black holes with various horizon topologies denoted by the parameter k, provided $\epsilon \equiv (k + m^2 c_2 c_0^2) > 0$ [85]. Taking the temperature T and thermodynamic volume V as the fluctuation variables, we computed the normalized Ruppeiner scalar curvature R_N and found novel behavior of microstructures at the HP transition point due the effect of graviton mass. Our findings are summarized below.

R_N diverges for the black hole with minimum temperature T_0. The small black hole branch is neglected as they are unstable, whereas for the large black hole branch, the nature of microstructures depends on the sign of R_N, which

in turn is governed by the sign of massive coefficient c_1. In the case when $c_1 \geq 0$ and for the large black hole branch,[4] R_N is negative indicating the dominance of attractive type interactions among the black hole microstructures. On the other hand when c_1 is negative, R_N can be positive, negative and also zero, from which one presumes the presence of repulsive, attractive, and vanishing interactions respectively, among the black hole microstructures. Interestingly, the microstructures in the zero temperature case are quite unique, in the sense that the value of the Ruppeiner scalar is $R_N = \frac{1}{2}$, which is independent of their horizon topology and also graviton mass, matching the claim of universal behavior made in the case of hyperbolic black holes [31].

R_N evaluated at the Hawking-Page transition point gives an intriguing dependence on pressure, which is unexpected, considering the recent proposal that R_N should probably be a universal constant at this point [27]. In the Schwarzschild-AdS black hole with spherical horizon topology ($k = +1$) and massless graviton case, R_N changes sign to negative at the HP transition point during the formation of stable black hole from thermal AdS. In massive gravity case with $c_1 \geq 0$ this still is the case. However, for $c_1 < 0$, R_N can be positive or zero, apart from being negative, showing a novel feature of black hole microstructures which is in contrast to massless graviton case (see Fig. 6). The zero of $R_N|_{HP}$ occurs at a critical pressure $p = p^* \equiv \frac{3c_0^2 c_1^2 m^4}{32\pi\epsilon}$ (or equivalently at a critical AdS length $l^* \equiv \frac{2\sqrt{\epsilon}}{c_0|c_1|m^2}$), such that the nature of interactions of microstructures are suggestively of attractive (repulsive) type for $p > (<) p^*$. Since the nature of microstructures varies with parameters, the formation of black holes in massive gravity theories is much more non trivial than the simple explanation of repulsive interactions shifting to attractive type at HP transition in Schwarzschild black holes in Einstein gravity [27]. Though the interactions of large black holes for non-zero graviton mass are repulsive type for small pressures, they are weaker than the microstructure interactions in the vacuum solution.

The strength of microstructure interactions at the HP transition (i.e., the magnitude $|R_N|_{HP}|$) depends on the topology parameter k and the massive gravity coefficient c_1. For $c_1 > 0$ one has,

$$|R_N|_{HP}|_{(k=-1)} > |R_N|_{HP}|_{(k=0)} > |R_N|_{HP}|_{(k=+1)}.$$

However, the order can be reversed, i.e., $|R_N|_{HP}|_{(k=-1)} < |R_N|_{HP}|_{(k=0)} < |R_N|_{HP}|_{(k=+1)}$, in the case of massive coefficient $c_1 < 0$, for some range of pressures as shown in Fig. 7.

[4]Here, the behavior of R_N with respect to massive coefficient c_1 for large black hole branch, is same as that of the corresponding branch in charged black hole case [22].

There are some special limits which are worth mentioning. The universal constant nature of Ruppeiner scalar curvature R_N at HP transition point [27] is broken due to the graviton mass and can be restored in a special limit of vanishing of the massive gravity coefficient c_1. This is a case where one takes the parameters, $k = 1$, $c_0 = 1$, $c_1 = 0$, and $c_2 = -1/2$ and the system under consideration was called the *holographic massive gravity model* of quantum field theories. Here, the breaking of diffeomorphism in bulk is due to the generation of effective graviton mass [105] leading to momentum dissipation in the field theory. In particular, there is a critical value of graviton mass where momentum dissipation effects are strong, leading to divergence of effective AdS length and also leading to a zero temperature confinement-deconfinement transition. We find that these phenomena persist in a more general case and also with hyperbolic topology [see Fig. 3(b)], where HP transition can happen at zero temperature when the graviton mass takes a critical value $\hat{m}^2 = -k/(c_2 c_0^2)$. $R_N^{(T_{HP}=0)}|_{HP}$ at $\hat{m}^2$ is a universal negative constant [independent of graviton mass, see Eq. (3.9)], taking exactly the same value found earlier for d-dimensional Schwarzschild black hole in AdS [27]. This intriguing result permits a speculation that the Ruppeiner scalar curvature R_N along the zero temperature confinement-deconfinement transition in dual field theory should also be a constant and also be independent of the momentum-dissipation rate, indicating the strongly correlated nature of microstructures. The universal behavior of microstructures at this special point deserves further study and it would be nice to directly compute R_N in a holographic dual model [105,123].

The geometry of the black hole close to the HP transition point was also explored in new double and triple near horizon scaling limits, respectively for the d-dimensional AdS Schwarzschild black hole and their counterparts in the massive gravity theory. In both the cases, with appropriate parameter choices, the presence of a fully decoupled Rindler space-time was seen, which is different from the standard near horizon geometry of general nonextremal black holes. A study of probe particles moving in the background of black holes in AdS at the HP transition point shows that the system is stable against small perturbations. Decoupled space times in the near horizon limits of extremal black holes and branes have opened up remarkable research in the AdS/CFT in past. It is hoped that the decoupled Rindler spacetimes found here would also turn out to be useful in developing holographic understanding of HP transition in near future.

ACKNOWLEDGMENTS

We thank the anonymous referees for helpful suggestions. One of us (C. B.) thanks the DST (SERB), Government of India, for financial support through the Mathematical Research Impact Centric Support (MATRICS) Grant No. MTR/2020/000135.

[1] S. W. Hawking and D. N. Page, Commun. Math. Phys. **87**, 577 (1983).
[2] D. Kastor, S. Ray, and J. Traschen, Classical Quantum Gravity **26**, 195011 (2009).
[3] B. P. Dolan, Classical Quantum Gravity **28**, 235017 (2011).
[4] A. Karch and B. Robinson, J. High Energy Phys. 12 (2015) 073.
[5] D. Kubiznak, R. B. Mann, and M. Teo, Classical Quantum Gravity **34**, 063001 (2017).
[6] A. Chamblin, R. Emparan, C. V. Johnson, and R. C. Myers, Phys. Rev. D **60**, 064018 (1999).
[7] M. M. Caldarelli, G. Cognola, and D. Klemm, Classical Quantum Gravity **17**, 399 (2000).
[8] D. Kubiznak and R. B. Mann, J. High Energy Phys. 07 (2012) 033.
[9] C. V. Johnson, Mod. Phys. Lett. A **33**, 1850175 (2018).
[10] G. Ruppeiner, Rev. Mod. Phys. **67**, 605 (1995); **68**, 313(E) (1996).
[11] R.-G. Cai and J.-H. Cho, Phys. Rev. D **60**, 067502 (1999).
[12] H. Quevedo, Gen. Relativ. Gravit. **40**, 971 (2008).
[13] A. Sahay, T. Sarkar, and G. Sengupta, J. High Energy Phys. 07 (2010) 082.
[14] S. A. Ho. Mansoori and B. Mirza, Phys. Lett. B **799**, 135040 (2019).
[15] M. Chabab, H. El Moumni, S. Iraoui, and K. Masmar, Eur. Phys. J. C **79**, 342 (2019).
[16] R. Banerjee, S. Ghosh, and D. Roychowdhury, Phys. Lett. B **696**, 156 (2011).
[17] K. Bhattacharya and B. R. Majhi, Phys. Rev. D **95**, 104024 (2017).
[18] S.-W. Wei, Y.-X. Liu, and R. B. Mann, Phys. Rev. Lett. **123**, 071103 (2019).
[19] Z.-M. Xu, B. Wu, and W.-L. Yang, Phys. Rev. D **101**, 024018 (2020).
[20] A. Ghosh and C. Bhamidipati, Phys. Rev. D **101**, 046005 (2020).
[21] A. N. Kumara, C. L. A. Rizwan, K. Hegde, M. S. Ali, and K. M. Ajith, Phys. Rev. D **103**, 044025 (2021).
[22] P. K. Yerra and C. Bhamidipati, Int. J. Mod. Phys. A **35**, 2050120 (2020).
[23] A. Dehyadegari, A. Sheykhi, and S.-W. Wei, Phys. Rev. D **102**, 104013 (2020).
[24] A. Dehyadegari and A. Sheykhi, arXiv:2107.02915 [Phys. Rev. D (to be published)].
[25] S.-W. Wei, Y.-X. Liu, and R. B. Mann, Phys. Rev. D **100**, 124033 (2019).
[26] J. Das Bairagya, K. Pal, K. Pal, and T. Sarkar, Phys. Lett. B **819**, 136424 (2021).
[27] S.-W. Wei, Y.-X. Liu, and R. B. Mann, Phys. Rev. D **102**, 104011 (2020).
[28] R. Emparan, J. High Energy Phys. 06 (1999) 036.
[29] J. F. Pedraza, W. Sybesma, and M. R. Visser, Classical Quantum Gravity **36**, 054002 (2019).
[30] C. V. Johnson and F. Rosso, Classical Quantum Gravity **36**, 015019 (2019).
[31] P. K. Yerra and C. Bhamidipati, Phys. Lett. B **819**, 136450 (2021).
[32] B. Wu, C. Wang, Z.-M. Xu, and W.-L. Yang, Eur. Phys. J. C **81**, 626 (2021).
[33] B. P. Abbott *et al.* (LIGO Scientific and Virgo Collaborations), Phys. Rev. Lett. **118**, 221101 (2017).
[34] C. de Rham, Living Rev. Relativity **17**, 7 (2014).
[35] G. Dvali, G. Gabadadze, and M. Porrati, Phys. Lett. B **484**, 112 (2000).
[36] G. Dvali, G. Gabadadze, and M. Porrati, Phys. Lett. B **485**, 208 (2000).
[37] B. P. Abbott *et al.* (LIGO Scientific and Virgo Collaborations), Phys. Rev. Lett. **116**, 061102 (2016).
[38] M. Fierz and W. E. Pauli, Proc. R. Soc. A **173**, 211 (1939).
[39] D. G. Boulware and S. Deser, Phys. Rev. D **6**, 3368 (1972).
[40] E. A. Bergshoeff, O. Hohm, and P. K. Townsend, Phys. Rev. Lett. **102**, 201301 (2009).
[41] C. de Rham, G. Gabadadze, and A. J. Tolley, Phys. Rev. Lett. **106**, 231101 (2011).
[42] C. de Rham, G. Gabadadze, and A. J. Tolley, Phys. Lett. B **711**, 190 (2012).
[43] Y. S. Myung, Y.-W. Kim, T. Moon, and Y.-J. Park, Phys. Rev. D **84**, 024044 (2011).
[44] E. A. Bergshoeff, O. Hohm, J. Rosseel, and P. K. Townsend, Phys. Rev. D **83**, 104038 (2011).
[45] W. Kim, S. Kulkarni, and S.-H. Yi, J. High Energy Phys. 05 (2013) 41.
[46] E. Ayón-Beato, M. Hassaïne, and M. M. Juárez-Aubry, Phys. Rev. D **90**, 044026 (2014).
[47] Y. S. Myung, Adv. High Energy Phys. **2015**, 478273 (2015).
[48] S. F. Hassan and R. A. Rosen, Phys. Rev. Lett. **108**, 041101 (2012).
[49] S. F. Hassan, R. A. Rosen, and A. Schmidt-May, J. High Energy Phys. 02 (2012) 26.
[50] Y.-F. Cai, D. A. Easson, C. Gao, and E. N. Saridakis, Phys. Rev. D **87**, 064001 (2013).
[51] H. Kodama and I. Arraut, Prog. Theor. Exp. Phys. **2014**, 023E02 (2014).
[52] D.-C. Zou, R. Yue, and M. Zhang, Eur. Phys. J. C **77**, 256 (2017).
[53] L. Tannukij, P. Wongjun, and S. G. Ghosh, Eur. Phys. J. C **77**, 846 (2017).
[54] T. Katsuragawa, S. Nojiri, S. D. Odintsov, and M. Yamazaki, Phys. Rev. D **93**, 124013 (2016).
[55] E. N. Saridakis, Classical Quantum Gravity **30**, 075003 (2013).
[56] Y.-F. Cai, C. Gao, and E. N. Saridakis, J. Cosmol. Astropart. Phys. 10 (2012) 048.
[57] G. Leon, J. Saavedra, and E. N. Saridakis, Classical Quantum Gravity **30**, 135001 (2013).
[58] K. Hinterbichler, J. Stokes, and M. Trodden, Phys. Lett. B **725**, 1 (2013).
[59] M. Fasiello and A. J. Tolley, J. Cosmol. Astropart. Phys. 12 (2013) 002.
[60] K. Bamba, M. W. Hossain, R. Myrzakulov, S. Nojiri, and M. Sami, Phys. Rev. D **89**, 083518 (2014).
[61] D. Vegh, arXiv:1301.0537.
[62] H. Zhang and X.-Z. Li, Phys. Rev. D **93**, 124039 (2016).
[63] J. Xu, L.-M. Cao, and Y.-P. Hu, Phys. Rev. D **91**, 124033 (2015).
[64] S. H. Hendi, B. E. Panah, and S. Panahiyan, J. High Energy Phys. 11 (2015) 157.
[65] S. Hendi, B. E. Panah, and S. Panahiyan, Classical Quantum Gravity **33**, 235007 (2016).

[66] S. H. Hendi, R. B. Mann, S. Panahiyan, and B. E. Panah, Phys. Rev. D **95**, 021501 (2017).
[67] S. Hendi, B. E. Panah, and S. Panahiyan, Phys. Lett. B **769**, 191 (2017).
[68] A. E. Gümrükçüoğlu, C. Lin, and S. Mukohyama, J. Cosmol. Astropart. Phys. 11 (2011) 030.
[69] P. Gratia, W. Hu, and M. Wyman, Phys. Rev. D **86**, 061504 (2012).
[70] T. Kobayashi, M. Siino, M. Yamaguchi, and D. Yoshida, Phys. Rev. D **86**, 061505 (2012).
[71] C. Deffayet, Phys. Lett. B **502**, 199 (2001).
[72] C. Deffayet, G. Dvali, and G. Gabadadze, Phys. Rev. D **65**, 044023 (2002).
[73] G. Dvali, G. Gabadadze, and M. Shifman, Phys. Rev. D **67**, 044020 (2003).
[74] G. Dvali, S. Hofmann, and J. Khoury, Phys. Rev. D **76**, 084006 (2007).
[75] C. M. Will, Living Rev. Relativity **17**, 4 (2014).
[76] M. Mohseni, Phys. Rev. D **84**, 064026 (2011).
[77] A. Gumrukcuoglu, S. Kuroyanagi, C. Lin, S. Mukohyama, and N. Tanahashi, Classical Quantum Gravity **29**, 235026 (2012).
[78] S. Hendi, G. Bordbar, B. E. Panah, and S. Panahiyan, J. Cosmol. Astropart. Phys. 07 (2017) 004.
[79] C. E. Rhoades and R. Ruffini, Phys. Rev. Lett. **32**, 324 (1974).
[80] B. E. Panah and H. L. Liu, Phys. Rev. D **99**, 104074 (2019).
[81] E. Babichev, L. Marzola, M. Raidal, A. Schmidt-May, F. Urban, H. Veermäe, and M. von Strauss, J. Cosmol. Astropart. Phys. 09 (2016) 016.
[82] Y. Akrami, T. S. Koivisto, and M. Sandstad, J. High Energy Phys. (2013) 99.
[83] Y. Akrami, S. F. Hassan, F. Könnig, A. Schmidt-May, and A. R. Solomon, Phys. Lett. B **748**, 37 (2015).
[84] C. Bachas and I. Lavdas, J. High Energy Phys. 11 (2018) 3.
[85] R.-G. Cai, Y.-P. Hu, Q.-Y. Pan, and Y.-L. Zhang, Phys. Rev. D **91**, 024032 (2015).
[86] L. Alberte and A. Khmelnitsky, Phys. Rev. D **91**, 046006 (2015).
[87] Z. Zhou, J.-P. Wu, and Y. Ling, J. High Energy Phys. 08 (2015) 67.
[88] A. Dehyadegari, M. K. Zangeneh, and A. Sheykhi, Phys. Lett. B **773**, 344 (2017).
[89] S. Hendi, B. E. Panah, S. Panahiyan, and M. Momennia, Phys. Lett. B **775**, 251 (2017).
[90] A. Dehghani and S. H. Hendi, Classical Quantum Gravity **37**, 024001 (2020).
[91] S. H. Hendi, S. Panahiyan, B. Eslam Panah, and M. Momennia, Ann. Phys. (Berlin) **528**, 819 (2016).
[92] A. R. Akbarieh, S. Kazempour, and L. Shao, Phys. Rev. D **103**, 123518 (2021).
[93] M. Högås and E. Mörtsell, arXiv:2106.09030.
[94] A. Caravano, M. Lüben, and J. Weller, J. Cosmol. Astropart. Phys. 09 (2021) 035.
[95] K. Hinterbichler, Rev. Mod. Phys. **84**, 671 (2012).
[96] R. A. Davison, Phys. Rev. D **88**, 086003 (2013).
[97] S. A. Hartnoll, C. P. Herzog, and G. T. Horowitz, Phys. Rev. Lett. **101**, 031601 (2008).
[98] S. A. Hartnoll, C. P. Herzog, and G. T. Horowitz, J. High Energy Phys. 12 (2008) 015.
[99] R. Gregory, S. Kanno, and J. Soda, J. High Energy Phys. 10 (2009) 010.
[100] L. Barclay, R. Gregory, S. Kanno, and P. Sutcliffe, J. High Energy Phys. 12 (2010) 029.
[101] L. Alberte and A. Khmelnitsky, Phys. Rev. D **91**, 046006 (2015).
[102] L. Alberte, M. Baggioli, A. Khmelnitsky, and O. Pujolas, J. High Energy Phys. 02 (2016) 114.
[103] L. Alberte, M. Ammon, A. Jiménez-Alba, M. Baggioli, and O. Pujolàs, Phys. Rev. Lett. **120**, 171602 (2018).
[104] H. Zhang, Y.-P. Hu, and Y. Zhang, Phys. Dark Universe **23**, 100257 (2019).
[105] A. Adams, D. A. Roberts, and O. Saremi, Phys. Rev. D **91**, 046003 (2015).
[106] S. H. Hendi, B. E. Panah, S. Panahiyan, H. Liu, and X. H. Meng, Phys. Lett. B **781**, 40 (2018).
[107] H. Zhang and X.-Z. Li, Phys. Rev. D **93**, 124039 (2016).
[108] O. Aharony, S. S. Gubser, J. M. Maldacena, H. Ooguri, and Y. Oz, Phys. Rep. **323**, 183 (2000).
[109] A. Belhaj, M. Chabab, H. El Moumni, K. Masmar, M. B. Sedra, and A. Segui, J. High Energy Phys. 05 (2015) 149.
[110] D. Birmingham, Classical Quantum Gravity **16**, 1197 (1999).
[111] G. Ruppeiner, Rev. Mod. Phys. **67**, 605 (1995).
[112] G. Ruppeiner, Phys. Rev. A **24**, 488 (1981).
[113] H. Janyszek, J. Phys. A, Math. Gen. **23**, 477 (1990).
[114] H. Janyszek and R. Mrugal/a, Phys. Rev. A **39**, 6515 (1989).
[115] H. Janyszek and R. Mrugaa, J. Phys. A, Math. Gen. **23**, 467 (1990).
[116] M. Cvetic, G. W. Gibbons, D. Kubiznak, and C. N. Pope, Phys. Rev. D **84**, 024037 (2011).
[117] L. D. Landau and E. M. Lifshitz, *Statistical Physics* (Elsevier Science, 1980), Vol. 5, https://books.google.co.in/books?id=D3zjAQAACAAJ.
[118] F. R. Tangherlini, Nuovo Cimento **27**, 636 (1963).
[119] S. H. Hendi, R. B. Mann, S. Panahiyan, and B. E. Panah, Phys. Rev. D **95**, 021501 (2017).
[120] P. K. Yerra and C. Bhamidipati, Classical Quantum Gravity **37**, 205020 (2020).
[121] S. Chandrasekhar, *The Mathematical Theory of Black Holes* (Springer Netherlands, Dordrecht, 1984), pp. 5–26.
[122] M. Olivares, J. Saavedra, C. Leiva, and J. R. Villanueva, Mod. Phys. Lett. A **26**, 2923 (2011).
[123] M. Alishahiha and A. Naseh, Phys. Rev. D **82**, 104043 (2010).